Groundwater and microbial processes of Alabama coastal plain aquifers

Elizabeth Penny and Ming-Kuo Lee

Department of Geology and Geography, Auburn University, Alabama, USA

Cynthia Morton

Carnegie Museum of Natural History, Pittsburgh, Pennsylvania, USA

Received 2 January 2003; revised 14 July 2003; accepted 28 August 2003; published 21 November 2003.

[1] We integrate groundwater geochemistry, microbiology, and numerical modeling techniques to study the origin of elevated salinity and chemical evolution of groundwaters in the coastal plain aquifers of Alabama. Our field data indicate that chemical composition of groundwater evolves by various geochemical and microbial processes as it moves deeper into the subsurface. Sequential peaks of Ca^{2+}, Mg^{2+}, K^{+}, and Na^{+} along flow paths indicate that separation of ions may be driven by cation exchange. Microbial-mediated reactions are important for the formation of several discrete hydrochemical zones containing Fe^{2+}, Mn^{2+}, Sr^{2+}, and SO_4^{2-} rich groundwaters. Elevated Fe^{2+}, Mn^{2+}, and Sr^{2+} concentrations may be derived from bacterial iron and manganese reduction. High sulfate concentrations observed a short distance from the recharge may be partly explained by microbial sulfur oxidation and nitrate reduction (denitrification). The presence of denitrifying and sulfur-oxidizing bacteria in water further supports these reactions. Major ion compositions and δD and $\delta^{18}O$ values are used to determine the source of salinity and the nature of mixing of different groundwaters. Three water types were identified; these include carbonate groundwater, brines associated with evaporites, and groundwater of meteoric origin. Groundwater age differences and flow velocities were calculated using the $^{36}Cl/Cl$ ratios. Calculated groundwater flow velocities within the Eutaw and Tuscaloosa aquifers are about 0.20 m/yr and 0.15 m/yr, respectively. We modeled basin-scale hydrologic and solute transport processes in a cross section extending from the aquifer outcrops to the Gulf Coast. The modeling result shows that the buried Jurassic Louann Salt can significantly increase groundwater salinity in the overlying coastal plain aquifers by density-driven advection and hydrodynamic dispersion. The modeling results are consistent with Cl/Br ratios and O/H isotope signatures, which indicate that salinity of the groundwater could be derived from seawater that has been evaporated beyond halite saturation. The predicted groundwater flow pattern reveals the mixing of meteoric water, carbonate groundwater (from the Ordovician Knox Group), and saline brines associated with the Louann Salt. The hydrologic model is consistent with the hydrochemical facies distribution in the Alabama coastal plain. *INDEX TERMS:* 1832 Hydrology: Groundwater transport; 1045 Geochemistry: Low-temperature geochemistry; 1065 Geochemistry: Trace elements (3670); 1040 Geochemistry: Isotopic composition/chemistry; *KEYWORDS:* groundwater, microbiology, hydrochemistry, isotopes, trace elements, coastal plain

Citation: Penny, E., M.-K. Lee, and C. Morton, Groundwater and microbial processes of Alabama coastal plain aquifers, *Water Resour. Res.*, *39*(11), 1320, doi:10.1029/2003WR001963, 2003.

1. Introduction

[2] The sources of salinity and chemical evolution of groundwater in sedimentary aquifers remain one of the most controversial problems in basin hydrology. Coastal plain aquifers in central south Alabama are exploited for large quantities of drinking water at depths, but groundwater is locally contaminated with trace elements including Fe and Mn (>300 ug/mg) and its chloride contents increase dramatically (>100,000 mg/kg) downdip. Although hydrochemistry and geology of coastal plain aquifers in Alabama have been studied by many investigators [e.g., *Knowles et al.*, 1963; *Scott et al.*, 1987; *King*, 1990; *Floesser*, 1996; *Cook*, 1993, 1997], the source of salinity and the influence of geochemical and microbial processes on groundwater chemistry remain poorly understood. Continuous increases in groundwater extraction from coastal plain aquifers have necessitated an evaluation of the origin of salinity and chemical evolution of groundwater supply in this region.

[3] Hydrogeologists have used different tools to construct the chemical evolution and hydrologic transport model for

0043-1397/03/2003WR001963$09.00

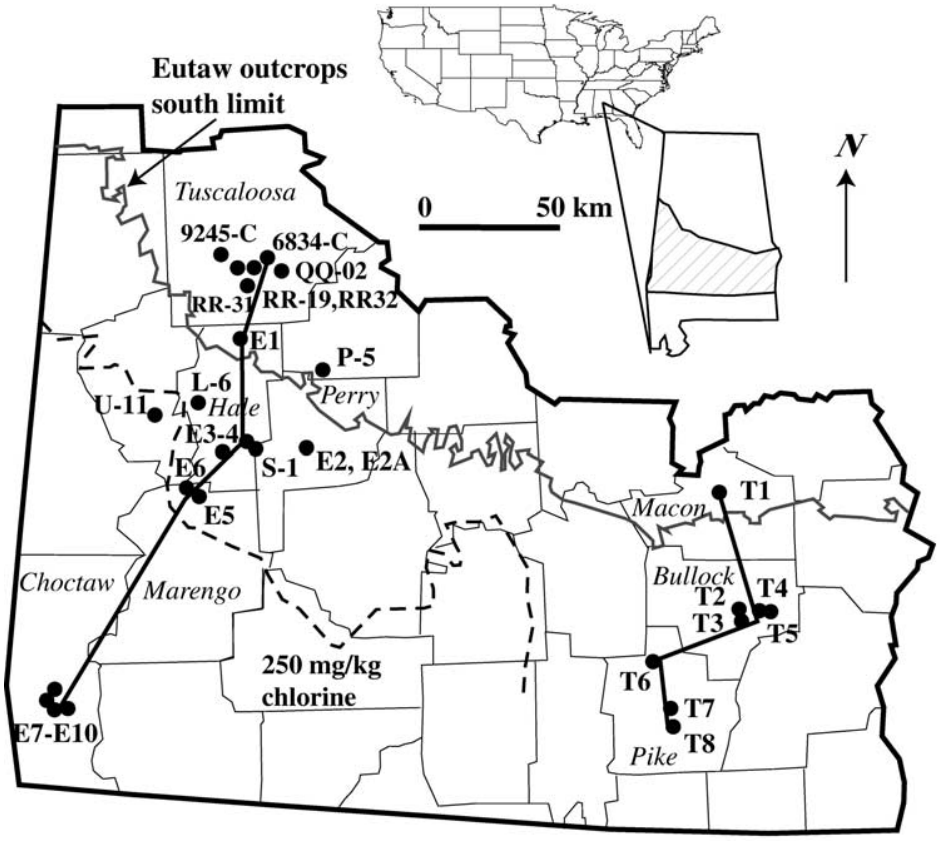

Figure 1. Location map of the investigated area in central south Alabama. Also shown are the southern limit of the recharge outcrop of the Eutaw aquifer (thin shaded line), contour line for equal Cl concentration of groundwater (250 mg/kg), and groundwater sampling locations (solid circles) and transects (thick lines) along (1) Macon-Bullock-Pike and (2) Tuscaloosa-Hale-Marengo-Choctaw.

regional groundwater systems. *Back and Hanshaw* [1970] introduced the hydrochemical facies concept to study the mixing of different groundwaters and water-sediment interaction along a flow path. Geochemists have since increasingly used the distribution and composition of stable isotope tracers to study groundwater sources and geochemical processes [*Clark and Fritz*, 1997]. Radioactive tracer techniques (e.g., ^{3}H, ^{36}Cl, $^{3}H/^{3}He$, $^{87}Sr/^{86}Sr$) have been widely used for estimating the residence time or age of groundwaters as well as their recharge and discharge rates [e.g., *Davis and Bentley*, 1982; *Bentley et al.*, 1986; *Lehmann et al.*, 1993; *Johnson et al.*, 2000; *Roback et al.*, 2001; *Alley et al.*, 2002]. In the past decade, newly developing nucleic-acid technology (see review by *Madsen* [2000]) allows scientists to investigate how microbial diversity and activity create discrete hydrochemical zones in regional aquifer systems [e.g., *Chapelle*, 1993; *Lovley and Chapelle*, 1995; *Jakobsen and Postma*, 1999]. Since then, the effect of microbial processes on chemical evolution of groundwater has been the subject of a large body of research. The nucleic acid probing and amplification method is especially useful in groundwater environments where the organisms of interest are usually present in relatively small number and traditional culture methods have not yet been successful. Because the mass transport processes are quite complex, scientists have come to rely on numerical modeling techniques to study how moving groundwater redistributes dissolved solutes. New hydrologic modeling tools which incorporate detailed hydrostratigraphic variations and geologic history have advanced our understanding of groundwater flow and solute transport processes in regional aquifer systems [*Bethke*, 1989; *Person et al.*, 1996; *Lee and Williams*, 2000]. The regional transport models have been used to study the origin of brines and the nature of salinity distributions observed in many sedimentary basins [e.g., *Ranganathan and Hanor*, 1987; *Garven et al.*, 1993].

[4] This study emphasizes the integrated approach by applying isotopic tracers, hydrochemistry, microbiology data, and numerical modeling in a regional-scale hydrogeology model. Data of major ions, trace elements, stable isotopes, radioactive isotopes, and the type of microorganisms were collected along two flow paths southward from outcrops of aquifers. The flow paths or general directions of groundwater flow were estimated from published potentiometric surfaces of regional aquifers in the study area [*Cook*, 1993]. Regional groundwater flow modeling was conducted to interpret the occurrence of brines and groundwater mixing in coastal plain aquifers. The results of numerical

modeling are integrated with geochemical and isotopic data to interpret the origin of salinity and chemical evolution of coastal plain aquifers in central south Alabama.

2. Geology and Hydrogeology

[5] The study area in central south Alabama belongs to the southeastern coastal plain province of the United States (Figures 1 and 2). The area is of moderate relief with surface elevations ranging from 200–300 m above sea level in the north to about 50–100 m in the south. The study area consists of unconsolidated Mesozoic and Cenozoic sediments unconformably overlying Precambrian to Paleozoic metamorphic and igneous rocks of the Alabama Piedmont province [*Horton et al.*, 1984; *King*, 1990]. The updip portion of coastal plain is a thick (>3000 m) wedge of sedimentary strata dipping south-southwest and trending approximately east-west and northwest-southeast (Figure 3). Table 1 shows the correlations of hydrostratigraphic and lithostratigraphic units in central south Alabama. These stratigraphic units consist of different sediment types with age ranging from Cambrian to late Paleocene.

[6] This study focuses on the hydrogeology and groundwater geochemistry of the Cretaceous Tuscaloosa and Eutaw aquifers. The Tuscaloosa Group is present in central south Alabama and crops out along the northern limit of the coastal plain. The thickness of the Tuscaloosa Group ranges from 200 to 400 m. The Tuscaloosa Group consists mainly of nonmarine deposits along the outcrops to marine clastics in the southern subsurface. West of the Tallapoosa River, the Tuscaloosa is divided into the Coker and Gordo Formations. The Tuscaloosa is not differentiated in eastern Alabama because of the absence of distinct marine deposits and fossils. The undifferentiated Tuscaloosa Group consists mainly of clay, fine to very coarse sand, and gravel.

[7] The Eutaw Formation consists of light to green-gray, cross laminated, fine to medium, well-sorted, micaceous, glauconitic sand [*Raymond et al.*, 1988; *King*, 1990]. The Eutaw Formation dips about 0.6 meter per kilometer with a thickness of a few meters at the northern part of the outcrop to 150 m near the Gulf coast. The Eutaw Formation is distinctly coarser and contains more marine glauconitic materials than the Tuscaloosa [*King*, 1990]. A clay zone separates the Eutaw Formation into the upper well-cemented sandstone and lower clay interbedded with sand. The upper confining units of the Eutaw aquifer, the Mooreville Chalk, Demopolis Chalk, and Blufftown Formation are low-permeability, micaceous and calcareous clays. The lower confining unit, the upper part of the Gordo Formation, is mostly clay.

[8] The Eutaw and Tuscaloosa aquifers are a major source of water supply for central south Alabama. Groundwater recharges along east-west and northwest-southeast outcrop trends in central Alabama (Figure 1). Groundwater migrates generally to the south in central east Alabama, and moves southwest in the western part of the study area, following the dip of the aquifers. Groundwater is pumped from the sandy portion of the aquifers throughout the northern part of the study area. Wells pumping potable groundwater from the Tuscaloosa aquifer are located as far south as central Pike County, about 70 km south of the outcrop area in south Alabama. In some locations, the continuous sand portion of these aquifers yields up to 1 million gallons (3780 m^3) of water per day [*Cook*, 1993]. Groundwater salinity increases southward and reaches several thousands of mg/kg in west-central Alabama and hundreds of thousands in southwest Alabama, whereas salinity of groundwater in eastern Alabama is mostly below 100 mg/kg. Why salinity is significantly higher in the western part of the study area is poorly understood. Abnormal salinity in western Alabama may be attributed to the presence of Louann Salt below the coastal plain aquifers [e.g., *Brobst et al.*, 1973; *Keller*, 2000] or a marine depositional environment.

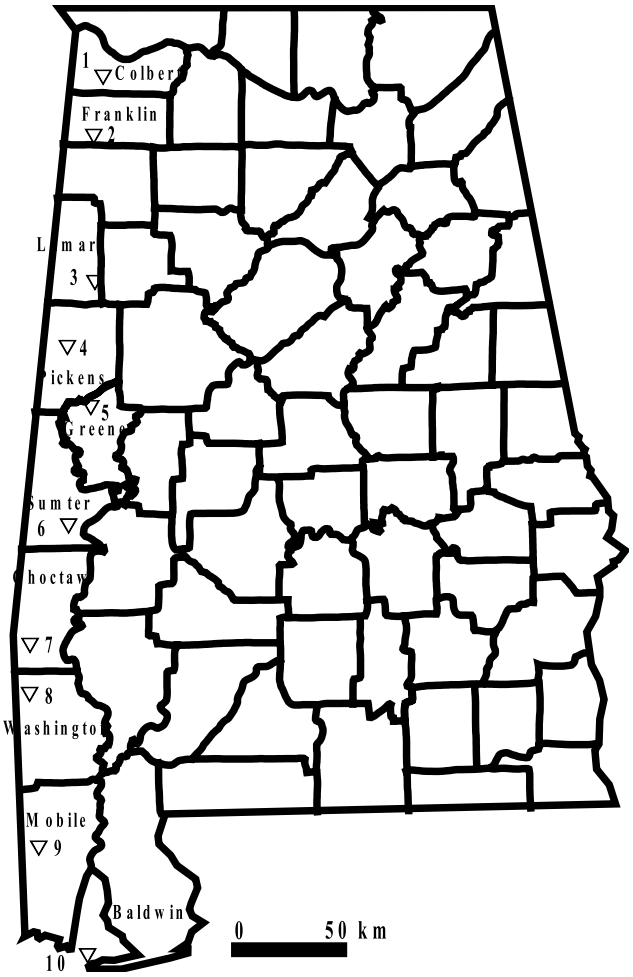

Figure 2. Location map of wells (1–10, open triangles) used to reconstruct the hydrostratigraphy of western Alabama in basin hydrology modeling (modified from *Raymond and Copeland* [1987]).

3. Methodology

3.1. Geochemistry Analysis

[9] Geochemical and isotope analyses have been conducted on groundwater samples taken along two transects (Figure 1) following flow lines southward from recharge areas in central Alabama. Major cations and stable isotopes (^{18}O and ^{2}H) analyses were conducted at the University of Arizona. Anions including Cl^-, Br^-, and SO_4^{2-} were

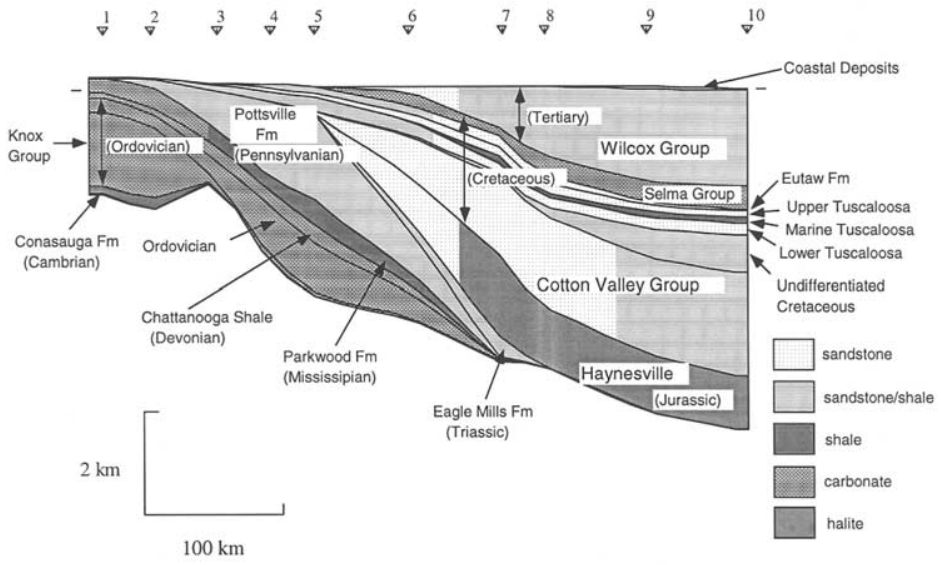

Figure 3. General hydrostratigraphic units in western Alabama used in the regional groundwater and solute transport modeling. The cross section is constructed based on geologic columnar sections from *Raymond and Copeland* [1987]. Well locations are shown in Figure 2.

analyzed at Los Alamos National Laboratory. Radioactive isotopes ^{36}Cl and ^{3}H compositions of groundwater samples were measured at the PRIME (Purdue Rare Isotope Measurement) Laboratory and U.S. Geological Survey (Menlo Park), respectively.

[10] All water samples but those from the Choctaw County were taken from municipal water supply. The Choctaw samples were collected from four industrial supply wells. To procure a sample that is representative of formation water, all wells were pumped continuously for at least

Table 1. Hydrostratigraphic and Lithostratigraphic Units From Recharge Area to Gulf Coast in Western Alabama

Hydrostratigraphy	System/Series	Lithostratigraphy
Coastal Deposits	Quaternary	coastal and low-level fluvial deposits, high-level fluvial deposits
Wilcox Group	Tertiary	Miocene undifferentiated, Pensacola Clay, Tampa Formation and Chickasawhay Limestone undifferentiated, Bucatunna Clay Member of Byram Formation, Jackson Group, Claiborne Group, Wilcox Group, Naheola Formation, Porters Creek Formation, Clayton Formation
Selma Group	Upper Cretaceous	Selma Group
Eutaw Formation	Upper Cretaceous	Eutaw Formation
Upper Tuscaloosa/Gordo	Upper Cretaceous	Gordo Formation or "upper Tuscaloosa"
Marine Tuscaloosa	Upper Cretaceous	"marine Tuscaloosa"
Lower Tuscaloosa/Coker	Upper Cretaceous	Coker Formation or "lower Tuscaloosa"
Undifferentiated Cretaceous	Upper Cretaceous	Lower Cretaceous undifferentiated, also Washita and Fredricksburg Groups undifferentiated
Cotton Valley Group	Lower Cretaceous	Paluxy Formation, Mooringsport Formation, Ferry Lake Anhydrite, Rodessa Formation, Silgo Formation, Hosston Formation, Cotton Valley Group
Haynesville Formation	Jurassic	Cotton Valley Group, Haynesville Formation, Buckner Anhydrite Member, Smackover Formation, Norphlet Formation, Pine Hill anhydrite, Louann Salt, Werner Formation
Eagle Mills Formation	Triassic	Eagle Mills Formation
Pottsville Formation	Pennsylvanian	Pottsville Formation, Parkwood Formation
Parkwood Formation	Mississippian	Parkwood Formation, Floyd Shale, Bangor Limestone, Hartselle Sandstone, Pride Mountain Formation, Tuscumbia Limestone, Fort Payne Chert
Chatanooga Shale	Devonian-Silurian	Chatanooga Shale, unnamed Devonian carbonate and chert unit, Sliurian undifferentiated, Wayne Group
Ordovician	Ordovician	Ordovician undifferentiated, Maysville and Nashville Groups undifferentiated
Knox Group	Cambrian-Ordovician	Knox Group undifferentiated, Ketona Dolomite
Conasauga	Cambrian	Conasauga Formation
Pre-Conasauga	Precambrian	basement complex

Table 2. Compositions of Selected Ions of Tuscaloosa and Eutaw Groundwater[a]

Sample	Well Name	Ca, mg/kg	Mg, mg/kg	Na, mg/kg	K, mg/kg	SO_4, mg/kg	Mn, ug/kg	Fe, ug/kg	Sr, ug/kg	pH	Alkalinity, mg/kg	TDS, mg/kg
						Tuscaloosa Aquifer						
T1	South Macon	43.5	1.7	9.4	4.3	18.0	3.9	0	195.0	7.55	142	224
T2	Union Springs 4	2.4	<0.5	51.4	<1	20.8	0.6	0	25.7	8.90	78	158
T3	Union Springs 3	1.0	<0.5	41.2	<1	13.8	0.1	0	7.4	9.04	54	115
T4	Layne3	1.4	<0.5	62.8	<1	45.5	0.1	0	11.5	9.06	52	170
T5	Smith 1	2.0	<0.5	78.6	<1	73.8	0.3	0	19.0	9.07	62	227
T6	Orion	<1	<0.5	66.1	<1	6.0	0.1	0	2.4	9.39	108	184
T7	Troy 6	<1	<0.5	107.0	<1	19.3	0.5	0	5.2	8.83	166	306
T8	Troy 8	<1	<0.5	79.0	<1	4.9	0.9	0	5.6	9.30	135	225
						Eutaw Aquifer						
E1	Moundville	1.1	0.7	1.5	2.9	2.3	0.1	0	12.9	5.55	5	15
E2	Marion-MMI	27.2	7.3	2.9	4.7	7.3	26.8	346	450.5	7.02	78	131
E2A	Marion-Plant	15.0	4.5	2.0	3.9	10.1	21.9	388	120.6	6.64	44	78
E3	Greensboro-CH	1.8	1.2	1.6	4.5	4.0	0.1	0	16.9	5.62	5	20
E4	Greensboro-Big	1.8	1.1	1.7	4.8	4.2	0.3	0	22.1	5.63	9	24
E5	Demopolis 5	1.1	<0.5	201.0	1.6	<0.2	7.6	478	97.4	8.66	265	574
E6	Demopolis 1	1.2	<0.5	213.0	<1	<0.2	8.8	338	118.6	8.72	279	600
E7	Morries 28-8	37300	3150	97320	5850	71750	7100	15000	2120000	5.48	6300	405700
E8	Skinner 30-10	35000	3100	96000	6350	82810	2900	10000	2100000	5.72	9800	402000
E9	Boney 33-8	2870	780	27360	120	1990	1300	10000	340000	6.41	760	82800
E10	Johnson	1870	640	19900	90	980	500	5000	220000	6.72	1200	60090

[a]Cl and Br concentrations are shown in Table 3.

one hour before sampling. A raw and an acidified sample from each well and their replicates were sent to ACTLABS for major ion and trace element analysis using inductively coupled plasma mass spectrometry (ICP-MS). Samples for trace element and cation analyses were passed through a 0.45 μm filter, acidified with concentrated HNO_3, and stored in polyethelene bottles. Temperature, pH, and electrical conductivity were measured in the field using hand-held water quality probes. Chloride and alkalinity concentrations were first measured in the field using standard titration methods. Chloride, bromide, and sulfate concentrations were measured in the laboratory using a Dionex 2000 ion chromatography. All samples were filtered prior to analysis using a 0.2 μm nylon filter. Precision of anion analyses is ±1% for chloride and sulfate, and ±3% for bromide. An $AgNO_3$ solution was added to the samples to precipitate AgCl for ^{36}Cl analysis. AgCl precipitates were purified by dissolution in NH_4OH and subsequently neutralized by HNO_3. A $Ba(NO_3)_2$ solution was also added to remove unwanted sulfur as $BaSO_4$. The procedure was repeated several times and the purified AgCl was oven-dried. A carrier was added to samples that contained very low concentrations of chloride. Stable isotopes ratios ($\delta^{18}O$ and δ^2H) were determined using the standard CO_2 equilibrium method. Results are reported in concentration units as per mil deviations from the SMOW standard [*Craig*, 1961]. The precision limits are ±0.2‰ for $\delta^{18}O$ and ±2‰ for δ^2H.

[11] The saturation indices (log Q/K) of carbonate minerals in groundwater were calculated using the Geochemist's Workbench [*Bethke*, 1996; *Lee and Bethke*, 1996]. The Geochemist's Workbench is one of a class of reaction path models that calculate the species distribution in aqueous solutions and traces chemical evolution of the systems involving fluids, minerals, and gases.

3.2. Microbial DNA Analysis

[12] Bacterial DNA extraction and sequencing were conducted at Auburn University to identify different microbial populations from selected hydrochemical zones where abnormal enrichments of Fe^{2+}, Mn^{2+}, and SO_4^{2-} are found. Microorganisms were filtered and their DNA extracted using an UltraClean Soil DNA Isolation kit (MOBIO laboratories, Inc.). Total DNA extracted was amplified using the Polymerase Chain Reaction (PCR) method [*Madigan et al.*, 1996]. Both the forward and reverse 16S rDNA universal primers were used for Bacterial and Archaeal domains [*Dojka et al.*, 1998]. The PCR products were used to create clone libraries in *E. coli*. Approximately 100 clones from each well site were subjected to Restriction Fragment Length Polymorphism (RFLP). RFLP data enable us to estimate the number of strains present and the majority at each site. The computer program Sequencher (Gene Codes Corporation version 3.0) was used to align raw sequencing data on a G3 Macintosh platform. Sequences were compared with all of the available sequences within the NCBI (National Center for Biotechnology Information) database for similarity using the BLAST (Basic Local Alignment Search Tool) network service.

3.3. Numerical Modeling

[13] Salinity distribution in the Tuscaloosa and Eutaw aquifers was modeled in two-dimension using a basin-scale groundwater flow model Basin2 [*Bethke et al.*, 1993; *Lee*, 1997]. The Basin2 model calculates groundwater flow resulting from density variation, sediment compaction, buoyancy, topographic relief, and the transport of heat, dissolved solutes, and noble gases in the basin strata. The partial differential equation for groundwater flow in a deforming two-dimensional medium is

$$\phi\beta\frac{\partial P}{\partial t} = \frac{\partial}{\partial x}\left[\frac{k_x}{\mu}\frac{\partial P}{\partial x}\right] + \frac{\partial}{\partial z}\left[\frac{k_z}{\mu}\left(\frac{\partial P}{\partial z} - \rho g\right)\right] - \frac{1}{(1-\phi)}\frac{\partial \phi}{\partial t} \quad (1)$$

here k_x and k_z are permeability (m^2), u is viscosity of fluid (kg $m^{-1}s^{-1}$), P is fluid pressure (kg $m^{-1}s^{-2}$), g is the

Table 3. The $^{36}Cl/Cl$, Cl, and Br Concentrations of Groundwaters in the Tuscaloosa and Eutaw Aquifers, Central South Alabama

Sample	Well Name	County	Distance From Recharge, km	Cl, mg/kg	Br, mg/kg	Cl/Br	$^{36}Cl/Cl$, $\times 10^{-15}$
			Tuscaloosa Aquifer				
T1	South Macon	Macon	5	4.55	0.02	256	156
T2	Union Springs 4	Bullock	30	5.14	0.03	166	144
T3	Union Springs 3	Bullock	32	4.01	0.03	153	134
T4	Layne 3	Bullock	40	7.63	0.07	110	119
T5	Smith 1	Bullock	40	9.98	0.05	180	113
T6	Orion	Pike	50	2.83	0.02	174	100
T7	Troy 6	Pike	70	12.99	<0.01	–	61
T8	Troy 8	Pike	70	4.52	0.05	84	58
			Eutaw Aquifer				
E1	Moundville 1	Hale	0	1.44	0.02	97	122
E2	Marion-MMI	Perry	15	2.32	0.02	104	105
E2A	Marion-Plant	Perry	15	4.22	0.01	340	44
E3	Greensboro-CH	Hale	20	1.74	0.01	149	95
E4	Greensboro-Big	Hale	20	1.72	0.09	195	91
E5	Demopolis 5	Marengo	50	104.53	0.95	109	8
E6	Demopolis 1	Marengo	50	106.35	0.98	108	6
E7	Morries 28-8	Choctaw	125	180,000	1,945	92	–
E8	Skinner 30-10	Choctaw	125	165,000	1,845	89	–
E9	Boney 33-8	Choctaw	125	48,500	242	200	–
E10	Johnson	Choctaw	125	35,000	185	188	–

acceleration due to gravity (m s^{-2}), β is fluid compressibility (m s^2 kg^{-1}), ϕ is porosity, and ρ is fluid density (kg m^{-3}). By equation (1), groundwater flow is driven by pressure compressing and density variation, rather than a combined form of hydraulic potential defined by *Hubbert* [1940].

[14] The Basin2 model also simulates diffusion, dispersion, and advection processes responsible for salinity distribution and solute transport. Basin2 calculates the distribution and transport of a solute in a groundwater system by solving the equation

$$\frac{\partial}{\partial t}(C) = \frac{\partial}{\partial x} D_x \left(\frac{\partial C}{\partial x}\right) + \frac{\partial}{\partial z} D_z \left(\frac{\partial C}{\partial z}\right) - q_x \left(\frac{\partial C}{\partial x}\right) - q_z \left(\frac{\partial C}{\partial z}\right) \tag{2}$$

where C is concentration (mol cm^{-3}), q is specific discharge (cm s^{-1}), t is time (s), and D is hydrodynamic dispersion (cm^2 s^{-1}), which accounts for molecular diffusion of solutes as well as mechanical dispersion. The model calculates the coefficients of hydrodynamic dispersion D_x and D_z from the following equations:

$$D_x = D^* + \alpha_L v_x' + \alpha_T v_z' \tag{3}$$

$$D_z = D^* + \alpha_L v_z' + \alpha_T v_x' \tag{4}$$

where D^* is the diffusion constant (cm^2 s^{-1}), α_L and α_T are the dispersivities (cm) in the longitudinal and transverse directions, and v_x' and v_z' are lateral and vertical fluid flow velocities (cm s^{-1}) in curvilinear coordinates. The program maps an irregular basin cross section into a finite difference grid. The x' direction lies along stratigraphic lines and hence curves to follow the dip of the basin strata. The z' direction is normal to x', or the stratigraphic lines. According to equations (3) and (4), the effect of dispersion is proportional to the flow velocity. Because the diffusion coefficient is relatively small ($\approx 10^{-6}$ cm^2 s^{-1}) with respect to dispersivities [*Freeze and Cherry*, 1979], the effects of dispersion usually dominate the solute transport processes even at modest flow rates ($>10^{-6}$ cm s^{-1} or a few meters per year).

4. Groundwater Geochemistry and Microbiology

[15] New and existing data of concentrations or trends of major and trace elements (Tables 2 and 3) were used to assess the fluid sources, mixing ratios, biochemical processes, and water-rock interaction history. Many previous studies [e.g., *Lee*, 1985; *Lovley and Chapelle*, 1995] found that redox potential of groundwater usually decreases along the flow path. The consumption of free oxygen by bacterially catalyzed reactions is followed by reduction of NO_3^-, reduction of MnO_2, and then reduction of ferric oxyhydroxides. When sufficiently negative redox levels have been reached, bacterial reduction of SO_4^{2-} to H_2S followed by reduction of organic matter to CH_4 will occur. In addition, *Chapelle and Knobel* [1983] and *Appelo* [1994] demonstrated that diagenetic reactions with carbonate minerals and cation exchange could result in systematic change of cation composition of groundwater along flow paths in coastal plain aquifers. The new geochemical data collected were compared to the theoretical electrochemical and chromatographic sequences.

4.1. Major Ions and Trace Elements

[16] Along the western transect, three major hydrochemical facies were identified, carbonate groundwater, saline groundwater associated with evaporites (sodium chloride), and groundwater of meteoric origin (Figure 4). The calcium bicarbonate facies was mostly found in coastal plain aquifers where deep groundwaters that migrated along faults discharge upward into Cretaceous aquifers (see discussion in section 6). Water samples contain significantly higher proportions of sodium and chloride likely derived from evaporated seawater (see following sections). Groundwaters with low major ion concentrations are largely meteoric

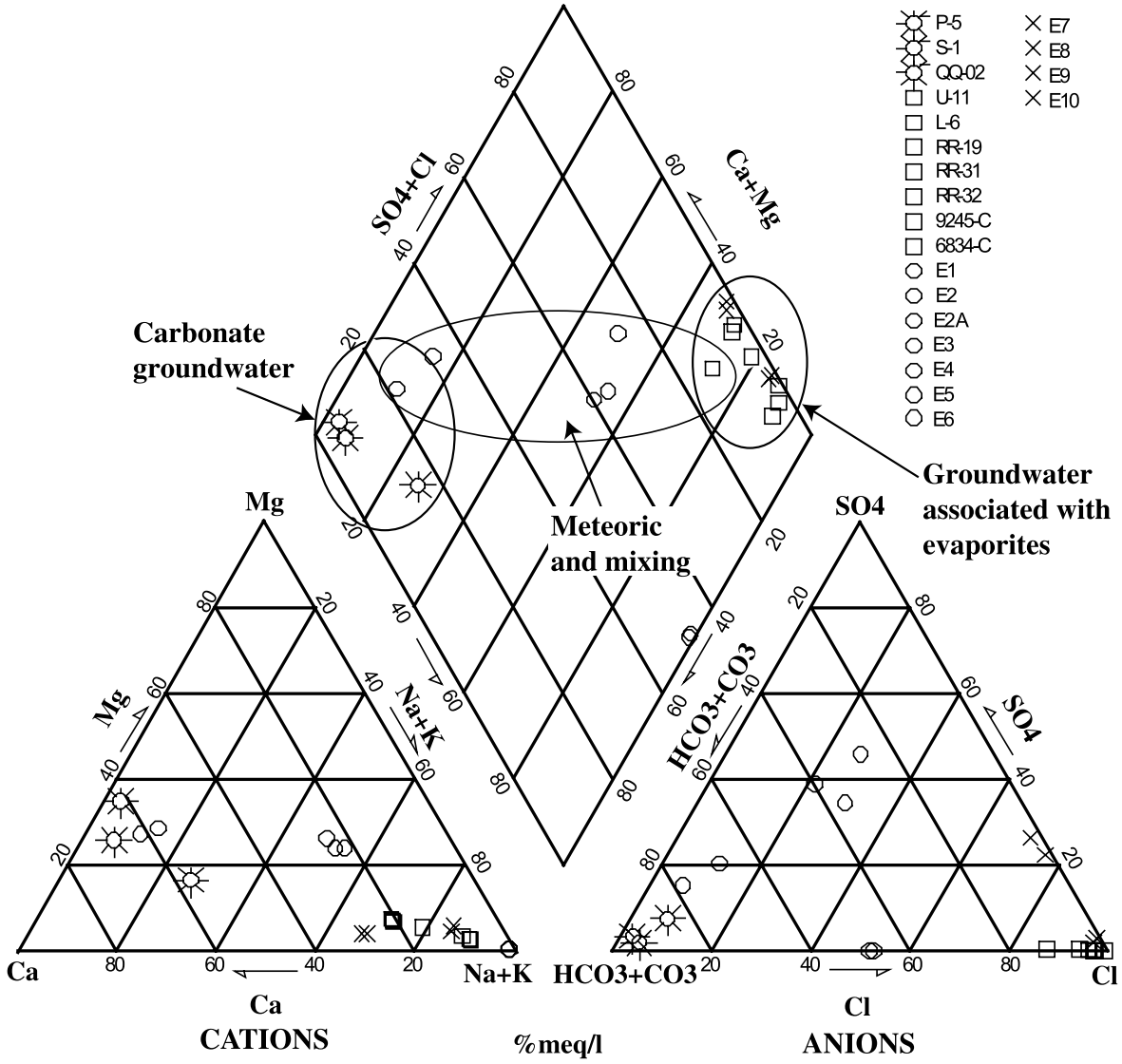

Figure 4. Piper diagram showing different hydrochemical facies from the Cretaceous aquifers in western Alabama, including carbonate groundwater, groundwater associated with evaporites, and meteoric water affected by the mixing of these two waters. Sample locations are shown in Figure 1.

water with some influence of the mixing of calcium bicarbonate and sodium chloride type groundwaters. In addition to physical mixing, the observed bulk water chemistry displays influence from cation exchange and microbial redox reactions.

[17] In western Alabama, significantly higher alkalinity and pH in the Marion and Demopolis wells (E2, E2A, E5, E6, Table 2) correspond to parallel spikes in Fe, Mn, and Sr concentrations (Figure 5). These correlations suggest that elevated Fe, Mn, and Sr concentrations may be derived from bacterial iron and manganese reduction similar to that proposed by *Saunders et al.* [1997] and *Zobrist et al.* [2000]:

$$4FeOOH_{(s)} + CH_2O + 7H^+ \rightarrow 4Fe^{2+} + HCO_3^- + 6H_2O \quad (5)$$

where CH_2O represents organic matter. This dissimilatory iron reduction would release metals and raise alkalinity of groundwater at the expense of H^+, organic carbon, and iron oxides. Concentrations of Sr also correlate well with dissolved Fe in the Ganges-Brahmaputra floodplain in the Bengal basin [*Dowling et al.*, 2003]. Recent experimental studies indicated that Sr can be sorbed to FeOOH solids and bacteria cell surfaces under oxidized conditions [e.g., *Small et al.*, 1999]. The sorbed Sr is subsequently mobilized when the redox conditions become favorable for bacterial iron reduction [*Roden et al.*, 2002; *Dowling et al.*, 2003]. Eh values of groundwater from Marion and Demopolis wells range from −5 to −50 mV; such slightly reducing conditions are favorable for bacterial iron reduction. Although coastal plain sediments contain abundant ferric oxyhydroxides [*Lee and Saunders*, 2003] and reduction of these solids is expected to generate large amounts of ferrous iron and alkalinity, the millimolar increase of alkalinity without concurrent increase in iron is not easily explained. The measured dissolved iron is less than 500 ug/l (0.01 mM)

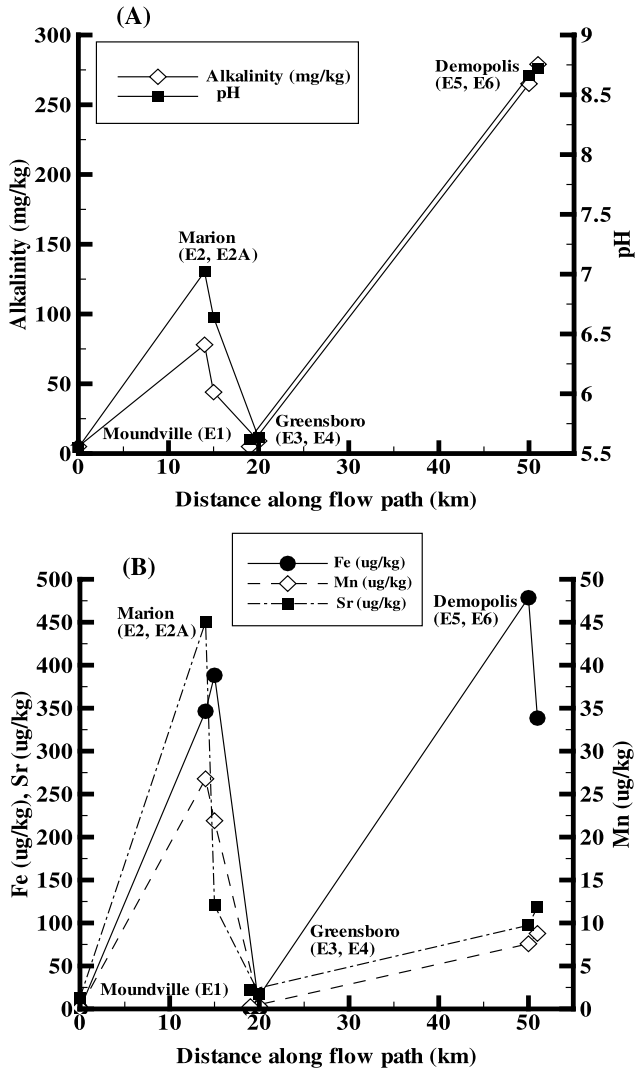

Figure 5. (a) Alkalinity and pH (Table 2) of groundwater samples at various distances from recharge along the transect (Figure 1) in western Alabama. (b) Fe, Mn, and Sr concentrations (Table 2) along the same transect.

and thus accompanying HCO_3^- increase would then be 0.0025 mM (0.15 mg/kg). Even when carbon-rich organic materials such as sucrose ($C_{12}H_{22}O_{11}$) are considered, the resulting alkalinity increase would be 0.03 mM (1.83 mg/kg) and significantly smaller than measured alkalinity (44–279 mg/kg, Table 2). The relatively high alkalinity could also be derived from inorganic sources such as calcite through dissolution or cation exchange reactions as suggested by *Chapelle and Knoble* [1983] and *Appelo* [1994]:

$$CaCO_3 + Na_2 - Ex + H^+ \rightarrow Ca - Ex + 2Na^+ + HCO_3^- \quad (6)$$

where Ex represents exchanging substrates. Downgradient from the recharge area, a sequence of Ca^{2+}, Mg^{2+}, K^+, and Na^+ dominated water along the western flow path (Figure 6) indicates that cation exchange could control the bulk water chemistry. In general, cations with small hydrated radii and higher charge tend to have higher affinity for exchange. The observed sequential peaks of cations are generally consistent with the order of cations competing for exchange sites: $Ca^{2+} > Mg^{2+} > K^+ > Na^+$. The sequences of Mg and Ca are not so widely separated (Figure 6) probably because both have two positive charges and are so similar in size. The cation exchange reaction (6) would produce a $NaHCO_3$ type water with high Na/Cl molar ratios (Tables 2 and 3).

[18] Groundwater samples collected along the eastern transect all have low TDS, <300 mg/kg (Tables 2 and 3), probably due to the lack of influence of buried evaporite beds that are present only in western Alabama [e.g., *Brobst et al.*, 1973; *Keller*, 2000]. High pH and alkalinity, as well as high Na contents without concurrent increase in Cl (Tables 2 and 3), again, indicate that the bulk water chemistry is highly influenced by cation exchange. Groundwater along the eastern transect is also influenced by biologically catalyzed reactions. High sulfate concentration along the aerobic portion of flow path near southern Macon County (wells T1–T5, Table 2) cannot be explained by remnant seawater because the SO_4/Cl molar ratios of groundwater (ranging from 1.27–2.73) are much higher than those of seawater (0.05). Sulfur oxidation and microbial nitrate reduction (denitrification) may be partly responsible for elevated sulfate contents. The amounts of O_2 dissolved in infiltrating water (about 5–6 mg/kg or 0.2 mM) can dissolve about 0.1 mM of pyrite or produce about 10 mg/kg of sulfate. This amount is close to those observed in wells T1, T2 and T3 but lower than elevated sulfate concentrations (up to 74 mg/kg) in wells T4 and T5, which are not easily explained. Alternatively, sulfate ions could be derived from surrounding confining layers by diffusion processes [*Hendry and Schwartz*, 1988]. The presence of chemolithotrophic bacteria *Thiobacillus* in the shallow Macon well T1 (see section 4.5) supports that bacterial oxidation of reduced sulfur might be an important source of

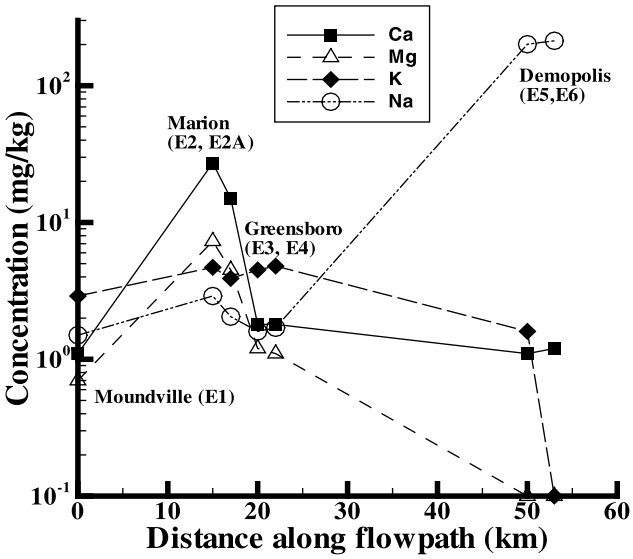

Figure 6. Concentrations of dissolved Ca, Mg, K, and Na in the Eutaw aquifer as function of distance along a flow path in western Alabama.

Table 4. Temperatures and Calculated Saturation Indices of Carbonate Minerals in Tuscaloosa and Eutaw Groundwaters Along the Flow Transect in Western Alabama

Sample	Well Name	Distance From Recharge, km	Temperature, °C	Saturation Indices			
				Calcite	Dolomite	Strontianite	Siderite
			Tuscaloosa Aquifer				
T1	South Macon	5	22.50	0.03	−0.23	0.17	−4.84
T2	Union Springs 4	30	25.78	0.02	−1.20	0.51	−1.63
T3	Union Springs 3	32	26.28	−0.30	−1.46	0.02	−1.58
T4	Layne 3	40	26.78	−0.13	−1.24	0.24	−3.55
T5	Smith 1	40	27.22	0.03	−1.08	0.45	−3.54
T6	Orion	50	34.00	−1.76	−2.29	0.02	−3.05
T7	Troy 6	70	31.50	−2.08	−2.97	0.04	−3.32
T8	Troy 8	70	34.28	−1.76	−2.28	0.39	−3.04
			Eutaw Aquifer				
E1	Moundville 1	0	20.11	−4.61	−8.30	−4.03	−7.90
E2	Marion-MMI	15	20.50	−0.77	−1.01	−0.03	−0.09
E2A	Marion Plant	15	21.11	−1.68	−2.77	−1.26	−1.49
E3	Greensboro-CH	20	22.11	−4.13	−7.34	−3.67	−7.62
E4	Greensboro-Big	20	21.78	−4.15	−7.42	−3.57	−7.64
E5	Demopolis 5	50	26.61	−0.11	−1.09	1.30	1.24
E6	Demopolis 1	50	24.78	−0.06	−1.02	1.45	1.09
E7	Morries 28-8	125	37.25	0.41	1.26	1.83	−1.32
E8	Skinner 30-10	125	37.10	0.95	2.35	2.35	−0.90
E9	Boney 33-8	125	36.50	0.27	1.44	1.86	−0.38
E10	Johnson	125	36.12	0.76	2.49	2.30	−0.02

sulfate in the groundwater. These sulfur-oxidizing bacteria can derive their energy and grow chemolithotrophically on reduced sulfur compounds [*Madigan et al.*, 1996]. In addition, the presence of denitrifying bacteria in the water (see section 4.5) suggests that some sulfate may be derived from the following biochemical reaction:

$$14\ NO_3^- + 5\ FeS_2 + 4\ H^+ \rightarrow 7\ N_2 + 10\ SO_4^{2-} + 5\ Fe^{2+} + 2\ H_2O \quad (7)$$

In this reaction denitrifying bacteria use reduced sulfur compounds (such as pyrite) as electron donors to transform nitrate. Because there are no significant mineralogical nitrate sources, bacterial denitrification cannot be the major process for generating elevated sulfate contents unless organic nitrate matter or anthropogenic sources such as sewage or agrochemicals are present. Further downdip to the south, the dramatic decrease of SO_4^{2-} and an increase in the "rotten egg" smell of H_2S in groundwater from south Macon to Troy (Table 2) indicates the bacteria reduction of sulfate in the deeper aquifer.

[19] We calculated the distribution of aqueous species in fluids and their saturation indices (S.I.) with respect to carbonate minerals at measured temperatures (Table 4). Most relatively shallow groundwaters in the Tuscaloosa aquifer (T1–T5) are slightly undersaturated or near equilibrium (S.I. ranges from −0.30 to 0.03) with respect to calcite. The deeper groundwater (T6–T8) near Troy are more undersaturated because dissolved Ca^{2+} is almost completely removed from aqueous solution by cation exchange reactions. Moundville water (E1) in the Eutaw aquifer is probably relatively recent meteoric water (pH = 5.55) that has had no significant contact with carbonate minerals; it is much more undersaturated with respect to carbonate minerals than other wells. The saturation states of calcite fluctuate along the Eutaw flow path (Table 4), reflecting various levels of alkalinity or Ca^{2+} concentrations influenced by cation exchange or microbial processes (i.e., equations 5 and 6). It should be noted that Fe-rich groundwaters in Demopolis and Marion are actually saturated with siderite ($FeCO_3$) and strontianite ($SrCO_3$), suggesting that reduced metal species also combine with HCO_3^- released from cation exchange or organic sources (equation (3)) to form carbonate minerals. Saline groundwaters in the Choctaw County originated from evaporated seawater (see sections 4.2 and 4.4) are supersaturated with most carbonate minerals.

4.2. Cl/Br Ratios

[20] Cl/Br ratios (Table 3) were used to determine the source of salinity in groundwater of the Eutaw aquifer in western-central Alabama. Different Cl/Br ratios have been observed in various natural waters [*Davis et al.*, 1998] including atmospheric precipitation (50–150), seawater and evaporated seawater (~290), and deep basin brine affected by congruent halite dissolution (>1000). The Cl/Br ratios of Eutaw aquifer samples range from 100 to 250, indicating that the groundwater has been influenced mostly by fresh water incursion and seawater evaporation, rather than congruent halite dissolution.

[21] The Cl/Br ratios of Eutaw groundwater (Figure 7) show a close correspondence with the seawater dilution and evaporation trajectory [*Carpenter*, 1978]. The origin and processes affecting salinity can be determined by the Cl/Br relationship to this trajectory (Figure 7). Cl/Br ratios remain constant during seawater evaporation until halite saturation is achieved, at which point Br is concentrated in the remaining solution, while Cl is removed by halite precipitation [*Connolly et al.*, 1990]. As a result, the Cl/Br ratio of the remaining brine decreases progressively during halite precipitation. Saline groundwaters derived from remnant evaporated brines beyond halite saturation generally exhibit Cl/Br ratios lower than seawater (i.e., to the right of the

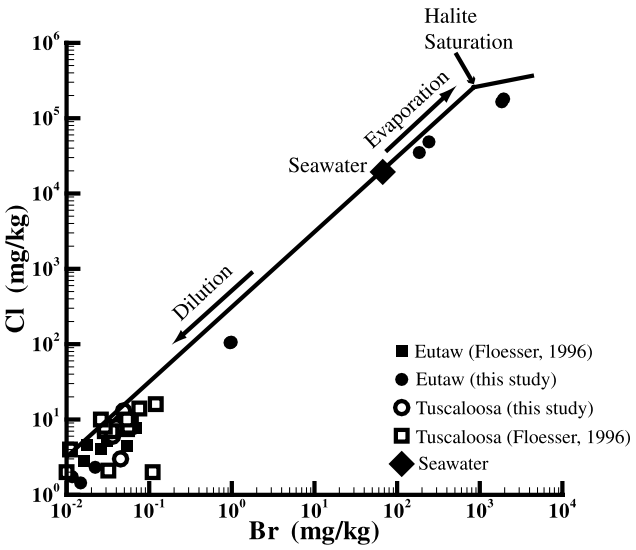

Figure 7. Cl/Br ratios of Eutaw and Tuscaloosa groundwater plotted along with the seawater evaporation trajectory [*Carpenter*, 1978]. Solid line shows trajectory of water evaporated towards the point of halite saturation. Solid line also shows the direction in which water moves as it is diluted by meteoric water. Eutaw groundwater samples that are considerably saline than seawater were collected from Choctaw County (E7–E10).

seawater evaporation trajectory) while congruent halite dissolution can produce groundwater with higher Cl/Br ratios (i.e., to the left of the seawater evaporation trajectory). The four brine samples from Choctaw County (E7–E10, Table 3) that are considerably more saline than seawater plot slightly to the right of the trajectory (Figure 7), indicating that they acquired salinity from remnant evaporite brines, rather than congruent dissolution of evaporite minerals. Dissolution of Louann Salt is therefore unlikely as a salinity source in the coastal plain aquifers since no Cl/Br ratios plotted above or to the left of the trajectory. The Cl/Br ratios of brine samples indicate that the salinity could be derived from seawater that has been evaporated beyond halite saturation and later diluted by subsequent meteoric water incursion. The Eutaw samples that are considerably more dilute than seawater have Cl/Br ratios lower than seawater, reflecting their meteoric origin. These samples fall slightly to the right or close to the conservative dilution line for seawater and meteoric water.

4.3. Radioactive Isotopes (^{36}Cl and ^{3}H)

[22] Radioactive isotopes data provide quantitative information on the age of groundwater (age between modern and several million years) and may be used to characterize current flow directions and velocities. Chlorine 36, with a half-life of about 300,000 years, can be used to date older groundwater [*Davis and Bentley*, 1982; *Bentley et al.*, 1986]. ^{36}Cl is formed naturally in the atmosphere by the bombardment of ^{40}Ar by cosmic-rays. Anthropogenic ^{36}Cl, however, has also been released into the atmosphere from nuclear explosions after 1952. All samples analyzed in this study have less than approximately 2 tritium units (TU), indicating that groundwater contains negligible anthropogenic ^{36}Cl. The ^{36}Cl method is most useful for dating groundwater that is significantly older (beyond the detection limit for ^{14}C) than that which can be dated with ^{14}C.

[23] ^{36}Cl/Cl ratios of groundwater in the Tuscaloosa and Eutaw aquifers range from 6×10^{-15} to 156×10^{-15} (Table 3). A high ^{36}Cl/Cl ratio near the recharge area corresponds to young groundwater with a strong atmospheric ^{36}Cl signature and gradually decreases moving away from the recharge area. Natural decay of ^{36}Cl with travel time in the aquifers is most likely responsible for the decrease of ^{36}Cl along the flow path. However, progressive mixing with old groundwater with little ^{36}Cl but high Cl concentrations at depths may be responsible for this decline (Figure 8). The low ^{36}Cl/Cl ratios of samples E5 and E6 from Demopolis wells suggest a very old chloride in the groundwater. For this reason, the ages of groundwater and brines downgradient from Demopolis wells (Cl > 100 mg/kg) cannot be determined using the ^{36}Cl/Cl method.

[24] If there are no additional sources for chloride in the groundwater system except for normal hypogene production, the age difference of two groundwater samples may be calculated using the following equation (modified from *Bentley et al.* [1986]):

$$\Delta t = t_1 - t_2 = \frac{-1}{\lambda_{36}} \ln \frac{R_1 - R_{se}}{R_2 - R_{se}} \qquad (8)$$

where λ_{36} is the decay constant of ^{36}Cl (2.3×10^{-6} yr^{-1}), R_1 and R_2 are the measured ^{36}Cl/Cl ratios for two groundwaters, and R_{se} is the secular equilibrium ratio controlled by hypogene production. This equation can be used to quantify the age difference and thus the average flow velocity (or recharge rate near outcrops) of groundwater between two locations without direct measurement of

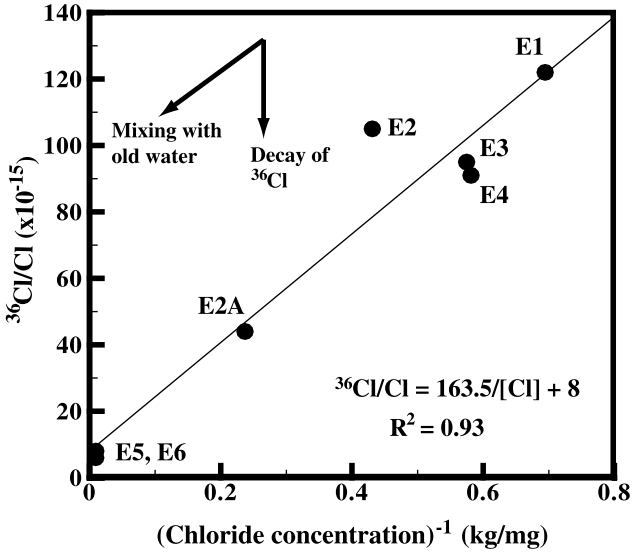

Figure 8. Regression curve for ^{36}Cl/Cl ratios and Cl concentrations of groundwater from the Eutaw aquifer in western Alabama. The two arrows represent radioactive decay and mixing of old groundwater that can change ^{36}Cl/Cl ratios and Cl concentrations.

Table 5. The δD and $\delta^{18}O$ Values of Groundwater in the Cretaceous Aquifers, Central South Alabama

Sample	County	Aquifer	δD, ‰	$\delta^{18}O$, ‰
T1	Macon	Tuscaloosa	−24	−4.7
T2	Bullock	Tuscaloosa	−22	−4.7
T3	Bullock	Tuscaloosa	−22	−4.7
T4	Bullock	Tuscaloosa	−22.5	−4.8
T5	Bullock	Tuscaloosa	−24	−4.7
T6	Pike	Tuscaloosa	−24	−4.8
T7	Pike	Tuscaloosa	−25	−4.8
T8	Pike	Tuscaloosa	−26	−4.9
9245-C[a]	Tuscaloosa	Pottsville	−25	−4.4
6834-C[a]	Tuscaloosa	Pottsville	−31	−3.7
RR-31[a]	Tuscaloosa	Coker	−33	−4.9
B-20[a]	Hale	Coker	−25	−4.9
L-6[a]	Hale	Lower Cretaceous	−32	−5.1
E0	Hale	Eutaw	−24	−5.0
E2	Perry	Eutaw	−21.5	−4.3
E6	Marengo	Eutaw	−24.5	−4.9
E7	Choctaw	Eutaw	−15	−2.3
E8	Choctaw	Eutaw	−10	2.9
E9	Choctaw	Eutaw	−19	−3.1
E10	Choctaw	Eutaw	−9	3.0
M1[b]	Lee	meteoric water	−93	−13
M2[b]	Lee	meteoric water	−37	−6.8
M3[b]	Lee	meteoric water	−16	−0.7

[a]Data from *Cook* [1997].
[b]Local meteoric water collected in Lee country, Alabama in January (M1), August (M2), and November (M3) during 2001.

$^{36}Cl/Cl$ ratios of an atmospheric recharge source. Using the parameters $R_{se} = 5.7 \times 10^{-15}$ from *Bentley et al.* [1986], the ^{36}Cl age difference of groundwater between Moundville (well E1) and Greensboro (well E4) is about 110,000 years. Given a flow path of 20 km, groundwater migrates at a rate of about 0.2 m/yr between these two wells in the Eutaw aquifer. The ^{36}Cl age difference of groundwater in South Macon (well T1) and Troy (well T8) is about 459,000 years. Thus groundwater travels at a rate of about 0.15 m/yr in the Tuscaloosa aquifer, close to the flow velocity in the Eutaw aquifer. It should be noted that the use of $^{36}Cl/Cl$ in groundwater dating must be viewed with caution because of uncertainty issues associated with groundwater mixing and carbonate diagenesis.

4.4. Stable Isotopes (δD/$\delta^{18}O$)

[25] δD and $\delta^{18}O$ values (Table 5) are used to determine the source of groundwater and its geochemical evolution in the coastal plain aquifers. Figure 9 shows δD and $\delta^{18}O$ ratios of groundwater relative to the seawater evaporation trajectory [*Holser*, 1979], the local meteoric water line, and the standard mean ocean water (SMOW). The local meteoric water line was constructed using rainwater data collected in this study (Table 5) as well as data from *Cook* [1997]. During evaporation, remnant seawater becomes progressively enriched in ^{18}O and ^{2}H relative to SMOW, as the light isotopes (^{16}O and ^{1}H) are preferentially concentrated in the vapor phase. However, with further evaporation beyond gypsum precipitation (4X) and toward halite saturation (∼10X), the residual brine becomes depleted in ^{18}O and ^{2}H due to mineral precipitation and isotopic fractionation. This hook-back trajectory explains why some basin brines could have lower δD and $\delta^{18}O$ values with respect to SMOW [*Stueber and Walter*, 1991]. Isotope ratios of Eutaw brines from Choctaw County (E7–E10, circles in Figure 9) fall along the mixing trends between the local meteoric water and evaporated seawater (Figure 9). The δD-$\delta^{18}O$ trend of brines intersects the evaporation trajectory at a point close to halite saturation (∼10X), which is consistent with the extent of seawater evaporation inferred from Cl-Br relations (Figure 7). Shallow Eutaw samples (circles in Figure 9) fall close to the local meteoric water line, indicating their common association with an atmospheric recharge source.

[26] Both δD-$\delta^{18}O$ and Cl-Br trends clearly indicate the mixing of remnant evaporated seawater (close to halite saturation) with meteoric water. Groundwater samples (9268-C, 6834-C, RR-31, B-20, L-6) of *Cook* [1997] collected to the north of the southern outcrop limit (Figure 1) display distinctively different δD and $\delta^{18}O$ values with respect to groundwater collected to the south. The groundwater likely originated from older Paleozoic carbonate rocks in the Alabama Valley and Ridge (Figure 2). The different isotope signatures may be attributed to different climate conditions at the time of recharge or through exchange of isotopes resulting from carbonate diagenesis. δD and $\delta^{18}O$ values of these samples, again, indicate three possible sources of groundwater. These include meteoric water, evaporated seawater (close to halite saturation), and groundwater from Ordovician/Devonian carbonate rocks.

4.5. Microorganisms

[27] Bacteria in SO_4^{2-}, Fe^{2+} and Mn^{2+} rich groundwater samples were filtered and identified using DNA sequencing

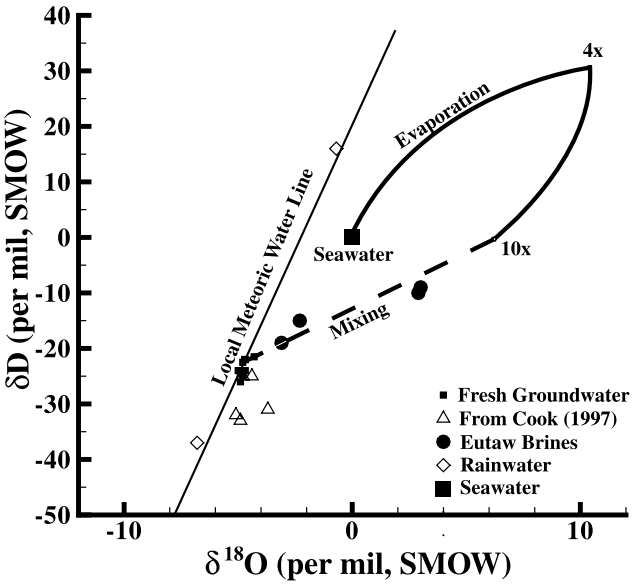

Figure 9. The δD and $\delta^{18}O$ ratios of Eutaw and Tuscaloosa groundwater plotted along with the seawater evaporation trajectory [*Holser*, 1979] and the local meteoric water line [*Cook*, 1997]. Shallow groundwater samples (solid squares, wells T1–T8, E1–E6) have isotopic compositions resembling that of local meteoric water. Isotope ratios of brines (solid circles, wells E7–E10) indicate that they were generated from mixing of evaporated seawater (10X, near halite saturation) with surface meteoric water. The isotopic compositions of water samples are shown in Table 5.

methods. Four different genera of bacteria, including *Burkholderia*, *Bacillus*, *Pseudomonas*, and *Thiobacillus*, were found in sulfate-rich water T1. *Burkholderia*, *Bacillus*, and *Pseudomonas* are major denitrifying bacteria [*Miller et al.*, 2002] and *Thiobacillus* can feed exclusively on iron and are capable of Fe^{2+} and Mn^{2+} oxidation [*Ariza*, 1998; *Bargar et al.*, 2000; *Malhotra et al.*, 2002]. *Thiobacillus* also utilizes the oxidation of inorganic sulfur sources to grow [*Madigan et al.*, 1996]. *Thiobacillus* is abundant in natural acid mine drainages such as the red Rio Tinto in Spain; some investigators believe that the low pH and elevated concentrations of metals in these extreme environments are produced by *Thiobacillus* [*Ariza*, 1998]. The presence of *Burkholderia*, *Bacillus*, *Pseudomonas*, and *Thiobacillus* suggests that bacteria sulfur oxidation and denitrification may be partly responsible for high sulfate concentrations in these groundwaters.

[28] *Pseudomonas* was found in Fe^{2+} and Mn^{2+} rich Eutaw groundwaters from Demopolis and Marion city wells. Both cities have to maintain expensive water treatment facilities to treat high-iron water. Previous pure batch culturing experiments have shown that *Pseudomonas* can utilize Fe(III) as terminal electron acceptors to grow in the absence of molecular oxygen [*Arnold et al.*, 1986]. Typical Fe(III) reducing bacteria include both strictly anaerobic (such as *Geobacter*) and facultative microbes (such as *Pseudomonas*) that survive in the presence of minor amount of oxygen [*Ehrlich*, 2002]. Most Fe-reducing microorganisms require sources of ferric iron and carbon to grow and metabolize. Fe (III) hydroxides (common in the coastal plain aquifer sediments) such as goethite, hematite, and ferrihydrite can be used as a ferric iron source for these organisms. Further work is needed to characterize the role of *Pseudomonas* in iron reduction and how various types of Fe(III) reducing bacteria [*Lovley et al.*, 1990; *Holmen et al.*, 1999] such as *Geobacter* may impact biogeochemical processes in the subsurface.

5. Basin Hydrology and Solute Transport Modeling

[29] Geochemical data presented in previous sections place compelling constraints on hypothesized processes for the mixing and origin of salinity of groundwater; further constraints may be provided by hydrologic transport modeling in the coastal plain aquifers. Variable-density groundwater flow and solute transport simulations were conducted in a cross section extending from the aquifer outcrops in western Alabama southward to the Gulf Coast. For the purpose of basin-scale hydrologic modeling, coastal plain strata in the study area are divided into eighteen hydrostratigraphic units (Table 1). Specifically, the simulations aim at evaluating (1) the effects of deep Louann Salt dissolution on groundwater salinity in the coastal plain aquifers and (2) the mixing of various ''end-member'' groundwaters in coastal plain aquifers. Geologic data from 10 deep wells [*Raymond and Copeland*, 1987, Figure 2] were used to reconstruct the hydrostratigraphy in the cross section (Figure 3). The hydrostratigraphic units of coastal plain aquifers in the calculations are composed of varying fractions of four types: sand, clay, carbonates, and evaporites (Figure 3). The cross section domain was divided into 30 columns vertically and 55 rows along stratigraphy in the finite difference grid. The columns have a uniform width (about 15 km) but the block height varies along the cross section with the thickness of the stratigraphic unit. Our basin-scale model assumes that the water table along the basin's top boundary lies at the land surface and the pressure along the water table is one atmosphere. The top surface of the basin is open to groundwater and subjected to freshwater recharge. The bottom of the cross section is set to be a no-flow boundary to reflect the low-permeability, Precambrian basement rocks. The left and right sides of the cross section remain open to groundwater flow. We calculate the evolution of porosity and permeability of each sediment buried, using correlation (Table 6) compiled by *Bethke et al.* [1993]. The diffusion coefficient D^* is assumed to be 1.5×10^{-5} cm^2 s^{-1} in the simulations. The values of dispersivity and permeability tend to increase with the scale of observation due to geologic heterogeneity [e.g., *Wheatcraft and Tyler*, 1988; *Gelhar et al.*, 1992], thus the variations in dispersivity and permeability represent sources of uncertainty in modeling salinity distribution within sedimentary basins. For sensitivity analyses, values of longitudinal dispersivity from 10 m to 1000 m, maintaining a dispersivity anisotropy of 10, are used in our models. These dispersivity values are in the same range as those used in the simulations of large-scale migration of contaminant plumes or brines [e.g., *Konikow and Bredehoeft*, 1974; *Domenico and Robbins*, 1985; *Person and Garven*, 1994]. Sensitivity analyses were also conducted to investigate how permeability variations (k = 0.1, 0.01, 0.001 darcy) may affect salt transport in coastal plain aquifers.

Table 6. Correlations Used in the Hydrologic Simulations to Calculate Porosity and Permeability of Basin Strata in the Alabama Coastal Plain

	Porosity[a]			Permeability[b]		
	ϕ_0	b, km^{-1}	ϕ_1	A	B	k_x/k_z
Sand	0.40	0.50	0.05	15	−3	2.5
Clay	0.55	0.85	0.05	8	−7	10
Carbonate	0.40	0.55	0.05	6	−4	2.5
Evaporite	0.55	0.85	0.05	0	−5	10

[a]Here $\phi = \phi_0 \exp(-bZ) + \phi_1$, expressed as a fraction; Z is burial depth (km).
[b]Here $\log k_x\ (\mu m^2) = A\phi + B$; $k_x \leq 1\ \mu m^2$; $1\ \mu m^2 \cong 1$ darcy.

5.1. Effects of Louann Salt

[30] A solute transport model was developed to examine how the buried Louann Salt might affect salinity in the coastal plain aquifers (Figure 10). The Louann Salt is part of the lower Jurassic and stratigraphically lies beneath thousands of meters of Cretaceous and other Jurassic strata. In the model, salinity along the basin surface was set to zero with no flux of salt across the basin's basal boundary. Groundwater within the Louann Salt maintains a salinity corresponding to halite saturation (about 6 molal). The model calculates a steady state solution for coupled groundwater flow and salt transport by advection, dispersion, and diffusion (see section 3). The use of steady state model is based on the assumption that the subsurface flow has adjusted over time to regional water table configuration and distribution of sediment permeability and the regional flow regime experienced little fluctuations over reasonable

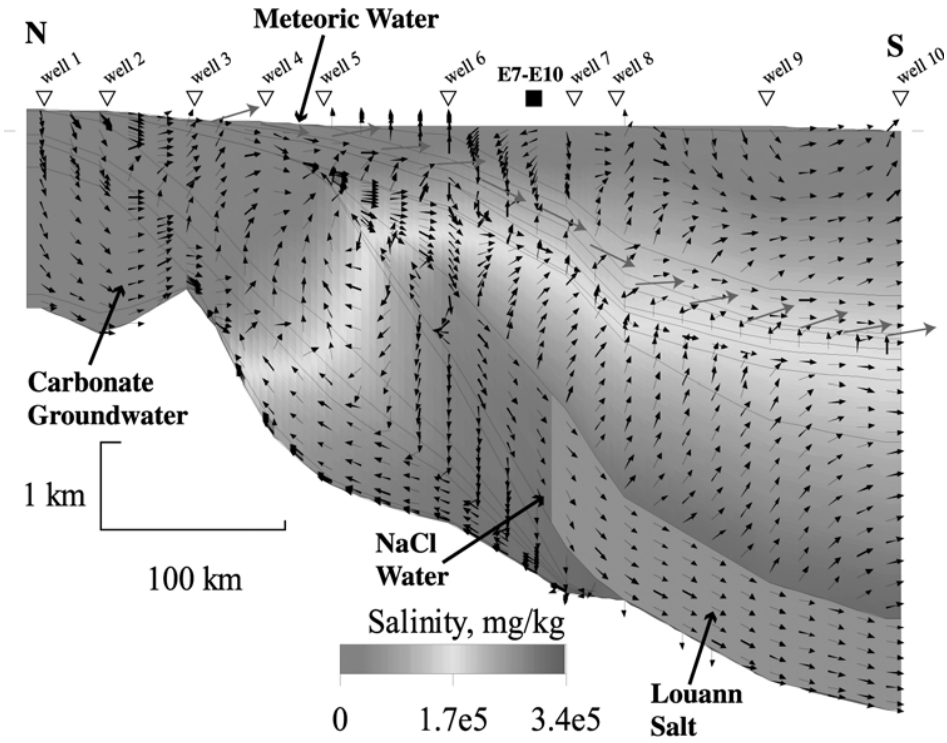

Figure 10. Solute transport model shows how the buried Louann Salt affects groundwater flow and salinity distribution in the Alabama coastal plain. Arrows are direction-only flow vectors. Large arrows highlight the flow directions in the Eutaw aquifer along the stratigraphy. Geologic well logs are marked by open triangles. The predicted flow pattern shows the mixing of meteoric water, carbonate groundwater, and saline brine associated with the Louann Salt. See color version of this figure in the HTML.

geologic time. The initial conditions were a hydrostatic distribution for pressure and a vertical diffusive gradient for salinity. In the simulations, the model proceeded to repeatedly solve the flow and mass transport equations until changes in pressure and concentration are within small tolerances for pressure (10^{-4} bar) and for salinity (10^{-4} molal). It usually took more than 300 iterations for our solute transport simulations to reach a convergence. The under-relaxation technique was used to limit the oscillations of variables over an iteration. We used a small under-relaxation parameter of 0.1 to reduce the correction made at each iteration, which avoid large oscillations and improve the overall convergence.

[31] Figure 10 shows the calculated steady state flow regime and the distribution of salinity in the cross section. The topographic relief across the basin surface provides the head for the regional flow regime and downward recharge of freshwater. The maximum flow velocity predicted by this model is on the order of 1.5 m/yr near the vicinity of outcrops. The calculated velocity decreases rapidly downstream from Moundville to less than a few tenths of meter per year. The decreasing flow velocities are consistent with field data that hydraulic gradients and hydraulic conductivity decrease rapidly down the dip of the Eutaw formation [*Cook*, 1993]. The calculated velocities downgradient from Moundville are within the same order of magnitude compared to those estimated by ^{36}Cl method, as discussed earlier.

[32] The results show that the Louann Salt can significantly increase groundwater salinity in the overlying coastal plain aquifers by density-driven advection and hydrodynamic dispersion (Figure 10). The large salinity variation creates a density flow, which carries salt toward the recharge area. Dispersion moves salt upward into the shallow strata where it is caught up in the southward flow of meteoric water. Thus the salt can advance and disperse laterally or vertically and result in an increase in fluid salinity upstream from the halite beds. When groundwater density varies along a stratigraphy direction l, the specific discharge q (cm s^{-1}) between two points in the formation is given by

$$q_l = -\frac{k_l}{\mu}\left[\frac{\partial P}{\partial l} - \rho g \frac{\partial z}{\partial l}\right] \tag{9}$$

Equation (9) implies that fluid flow must take place anytime ($q_l \neq 0$) if a lateral density gradient exists along stratigraphy. *Deming* [2002] indicated that the head difference Δh between two points along a stratigraphy line may be calculated as

$$\Delta h = \frac{P_1 - P_2}{\rho_a g} = \frac{\rho_1 z_1 - \rho_2 z_2}{\rho_a} \tag{10}$$

where ρ_1 and ρ_2 are the average fluid density above points 1 and 2, respectively, and $\rho_a = (\rho_1 + \rho_2)/2$. If we assume a

depth of 5000 m ($z_1 = z_2 = 5000$ m), $\rho_1 = 1100$ kg m^{-3}, and $\rho_2 = 1000$ kg m^{-3}, the result Δh between two points is about 475 m. Groundwater would migrate from point 1 to point 2 in response to this lateral density gradient. Moreover, the average flow velocity between these two points is

$$v = -\frac{k\rho_a g}{\mu\phi}\frac{\Delta h}{\Delta l} \quad (11)$$

If we further assume a typical formation permeability k of 10^{-15} m^2, fluid viscosity μ of 10^{-3} kg m^{-1}s^{-1}, a porosity ϕ of 0.1, and a lateral migration distance Δl of 10 km, the flow velocity v driven by density variation is about 0.15 m per year. It would take about 66 k.y. for the denser fluid at point 1 to replace fluids at point 2. Specifying more concentrated brines and more permeable basin strata would increase the flow velocity and solute transport. Although the magnitude of density-driven flow is relatively small in comparison to those of topographic-driven flow (usually on the order of meters or tens of meters per year), the cumulative effects of slow solute transport processes could significantly raise groundwater salinity over geologic time. Our modeling result (Figure 10) suggests that the Louann Salt could create large variations in fluid salinity, which in turn leads to density-driven fluid flow and upstream salt transport in the Alabama coastal plain. *Ranganathan and Hanor* [1987] studied the effects of a buried halite layer on the salinity distribution in sedimentary basins. Their results also show that upward advection and dispersion of salt could form very salty pore waters in overlying strata.

[33] On the basis of Cl/Br and stable isotope signatures (Figures 7 and 9), salinity of the Eutaw groundwater could be derived from seawater that has been evaporated beyond halite saturation. However, the salinity could not be derived directly from congruent halite dissolution, which would produce much higher Cl/Br ratios (>1000) than those observed in the field (50–200). The elevated salinity in groundwater more likely comes from the deep buried brines reaching halite saturation, in close association with the Louann Salt. Our field data (Table 3) show that groundwater salinity quickly increases and exceeds that of seawater at distances >100 km to the south of the recharge zone (i.e., downdip from the Choctaw County). The low Cl/Br ratios and elevated salinity imply that the extent to which freshwater can infiltrate downdip toward the deep Louann salt is quite limited. The deep freshwater incursion is limited by the flat hydraulic potentials [*Miller*, 1990; *Cook*, 1993] and the presence of dense brines in southern Alabama coastal plain. The upstream migration of dense brines (Figure 10) could also counter-act the downdip freshwater incursion.

[34] A series of three simulations illustrate the effects of dispersivity on salinity distribution in the Eutaw aquifer (Figure 11a). At steady state the infiltrating freshwater increases in salinity along its flow path due to the upstream solute transport from the deep Louann Salt. Different values of dispersivity (α_L = 10, 100, and 1000 m) form a broad range of salinity and a higher degree of dispersion tends to raise water salinity in the overlying aquifers under the same hydrologic conditions. While our interpretive models pro-

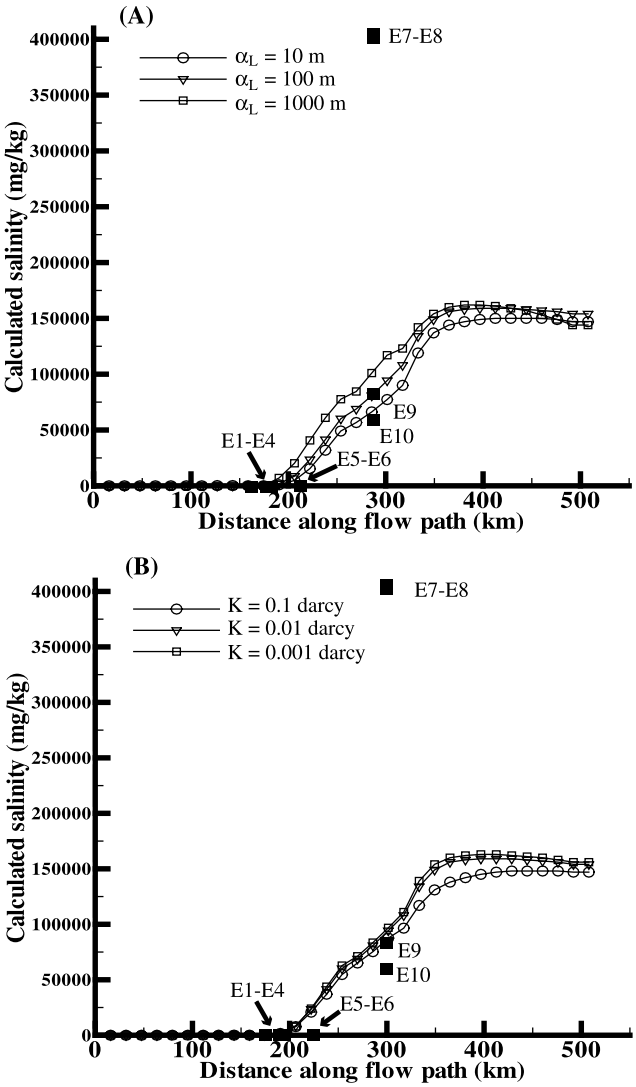

Figure 11. Calculated effects of (a) longitudinal dispersivity (α) and (b) permeability (k) on salinity distribution along a flow path (flow directions are indicated by large arrows in Figure 10) in the Eutaw aquifer. Solid squares represent observed concentrations of groundwater (E1 and E10) collected along the flow path (Figure 1).

vide important insights into the rates and migration patterns of fluids and solutes on a regional scale, much work remains to be done toward the prediction of salinity distribution. The calculated range of salinity in the Eutaw aquifer is consistent with brine concentrations observed in wells E9 and E10 (60,000–82,000 mg/kg) but compares poorly with near-by wells E7 and E8 (~400,000 mg/kg) of the Choctaw County (Figure 11). The large increase of water salinity in wells E7 and E8 may be the results of facies change and differing stratigraphic setting over a short distance, which is a common geologic phenomenon in coastal plain environments. The presence of local low-permeability zones such as shale partings and interlayered shale could trap original brines while permeable sandy lens provide preferential flow paths for groundwater flushing [*Lee et al.*, 2000]. Incorporating local heterogeneities is among the major challenges

and uncertainties in basin hydrologic modeling since the local behavior may deviate significantly from average properties of the same basin strata on the regional scale of interest.

[35] Our sensitivity analyses also explored how variations in sediment permeability may affect solute transport in the Eutaw aquifer. In three sets of numerical experiments, the Eutaw aquifer had constant permeability values of 0.1, 0.01, and 0.001 darcy (1 darcy = 10^{-8} cm^2), respectively. The dispersivity α_L and α_T were held constant as 100 m and 10 m in these simulations. A reduction in permeability would reduce both the extent of freshwater incursion and upstream solute dispersion by lowering the groundwater velocity. The calculated salinities show little variations at distances less than about 200 km from the recharge (Figure 11b) because the changes of freshwater incursion and solute dispersion cancel out each other. However, specifying lower permeability yields higher solute concentrations further downstream near the salt source (>300 km) where diffusion dominates solute transport at very low flow rates. Our sensitivity analyses show that variations in dispersivity and permeability would affect the solute concentrations to some extent, but not the occurrence of brines in the southern coastal plain. While it is still a long way off for the development of three-dimensional basin models fully accounting for all coupling hydrogeologic processes and sub-basin scale heterogeneities, our regional hydrologic model should be viewed most of its use in calculating "order of magnitude" estimates of flow rates and solute transport processes.

5.2. Groundwater Mixing Model

[36] The predicted flow pattern (Figure 10) reveals the possible mixing and interaction between meteoric recharge and groundwater associated with Knox Group carbonate strata (Ordovician) and Louann Salt. The Tuscaloosa and Eutaw sands serve as major regional aquifers for southward flow of meteoric water. Near the northern portion of the coastal plain, groundwater migrating in the Ordovician Knox Group carbonate strata discharges upward along the basement high, probably through faults and fractures in Paleozoic rocks [*Cook*, 1997], into the overlying Cretaceous aquifers. The carbonate groundwater then mixes with meteoric water in the shallow aquifers and continues to migrate southward. This flow pattern is consistent with the hydrochemical facies distribution in the northern coastal plain, which suggests widespread mixing of carbonate groundwater (e.g., wells P-5, S-1, and QQ-02 in Figures 1 and 4) with meteoric water.

[37] The calculated results (Figure 10) demonstrate the effects of Louann Salt on the salinity of the groundwater in Alabama coastal plain aquifers. Salinities are generally low in the northern recharge area but high in the southern coastal plain, especially at depth within and adjacent to the Louann Salt. Shallow groundwater driven by topography migrates downward and mixes with saline brines associated with the Louann Salt, and then flow toward the Gulf Coast under the regional hydraulic gradient. The high brine density causes groundwater to sink along the northern edge of the salt (at depth between wells 6 and 7) and then carry salt back toward the northern coastal plain. This density driven groundwater then mixes with shallow groundwater and causes an increase in fluid salinity upstream from the Louann Salt (e.g., wells U-11, L-6, RR-19, and 9245-C in Figures 1 and 4).

6. Conclusions

[38] This research correlates hydrologic, geologic, geochemical and microbial data to develop an integrated reactive transport model for water, solutes, isotopes, and microbes in coastal plain aquifer systems. Detailed field data and numerical models were used to understand relations among groundwater geochemistry, isotope hydrology and microbiology. The results indicate that chemical composition of groundwater evolves by mechanic mixing, cation exchange, and biochemical processes as it moves deeper into the subsurface.

[39] The three water types that were identified are carbonate groundwater, groundwater associated with evaporates, and groundwater of meteoric origin. Discrete hydrochemical zones with distinct major ion and trace element compositions are maintained by cation exchange, carbonate dissolution, and microbial processes. Peaks of Ca^{2+}, Mg^{2+}, K^+, and Na^+ are spatially separated along the flow path as the coastal plain aquifers are subject to freshwater flushing and cation exchange processes. Cation exchange processes also lead to significantly elevated alkalinity and pH values of groundwater. Elevated Fe, Mn, and Sr concentrations may be derived from bacterial iron and manganese reduction. High sulfate concentrations in shallow wells may be partly explained by oxidation of reduced sulfur and microbial denitrification. The presence of denitrifying bacteria *Burkholderia*, *Bacillus*, and *Pseudomonas* as well as sulfur oxidizing bacteria *Thiobacillus* in shallow water further supports this model. The dramatic decrease of SO_4^{2-} and smell of H_2S in groundwater southward from Macon to Pike County indicate that the deeper groundwaters are affected by the bacterial reduction of sulfate.

[40] Cl/Br ratios and δD and δ^{18}O values were used to determine the source of salinity and the nature of mixing of groundwaters. Both δD-δ^{18}O and Cl-Br trends indicate the mixing of remnant evaporated seawater (close to halite saturation) with meteoric water. Groundwater age differences and flow velocities were calculated using the ^{36}Cl/Cl ratios. Calculated groundwater flow velocities in the Eutaw and Tuscaloosa aquifers are 0.2 m/yr and 0.15 m/yr, respectively.

[41] Basin-scale hydrologic transport models were developed in a cross section extending from the aquifer recharge zones to the Gulf Coast. The solute transport model shows that the buried Jurassic Louann Salt can significantly increase groundwater salinity in the overlying coastal plain aquifers by density-driven advection and dispersion. The modeling results are consistent with Cl/Br ratios and stable isotope signatures, both indicating that salinity of the groundwater could be derived from seawater that has been evaporated beyond halite saturation. Sensitivity analyses show that salinity distribution depends on assumptions of dispersivity and permeability. The predicted salinity in the shallow aquifers increases with increasing solute dispersion from the underlying Louann Salt. Lower permeability yields higher solute concentrations at depths near the salt source where diffusion dominates solute transport at very low flow rates. The predicted groundwater flow pattern reveals the mixing of meteoric water, carbonate groundwater (from the

Ordovician Knox Group), and saline brines associated with Louann Salt. The hydrologic model is consistent with the hydrochemical facies distribution in the Alabama coastal plain.

[42] **Acknowledgments.** This research was supported by grants from the Gulf Coast Association of Geological Societies (to Elizabeth Penny), the USGS-AWRRI Program (to L. W. Wolf, J. A. Saunders, and M.-K. Lee), and by the Petroleum Research Fund, administered by the American Chemical Society under ACS-PRF 37071-AC2 (to Ming-Kuo Lee). We thank Marlon Cook and Charles Smith for many helpful discussions on hydrogeology and stratigraphy of the study area. A portion of the chemical and isotopic data was collected from a separate study of the geographic variations of chlorine 36 in groundwater. Stanley N. Davis cooperated with us in this work and his assistance is gratefully acknowledged. This paper has greatly benefited from constructive comments from Fiona Whitaker and one anonymous reviews.

References

Alley, W. M., R. W. Healy, J. W. LaBaugh, and T. E. Reilly, Flow and storage in groundwater systems, *Science*, *296*, 1985–1990, 2002.

Appelo, C. A. J., Cation and proton exchange, pH variations, and carbonate reactions in a freshing aquifer, *Water Resour. Res.*, *30*, 2793–2805, 1994.

Ariza, L. M., River of vitriol, *Sci. Am.*, *26*, 26–28, 1998.

Arnold, R. G., T. M. Olson, and M. R. Hoffmann, Kinetics and mechanism of dissimilative Fe(III) reduction by *Pseudomonas* sp. 200, *Biotech. Bioeng.*, *28*, 1657–1671, 1986.

Back, W., and B. B. Hanshaw, Comparison of chemical hydrogeology of the carbonate peninsulas of Florida and Yucatan, *J. Hydrol.*, *10*, 330–368, 1970.

Bargar, J. R., B. M. Tebo, and J. E. Villinski, In situ characterization of Mn(II) oxidation by spores of the marine *Bacillus* sp. strain SG-1, *Geochim. Cosmochim. Acta*, *64*(16), 2775–2778, 2000.

Bentley, H. W., F. M. Phillips, S. N. Davis, M. A. Habermehl, P. L. Airey, G. E. Calf, D. Elmore, H. E. Gove, and T. Torgersen, Chlorine 36 dating of very old ground water: 1, The Great Artesian basin, Australia, *Water Resour. Res.*, *22*, 1991–2001, 1986.

Bethke, C. M., Modeling subsurface flow in sedimentary basins, *Geol. Rundsch.*, *78*, 129–154, 1989.

Bethke, C. M., *Geochemical Reaction Modeling*, Oxford Univ. Press, New York, 1996.

Bethke, C. M., M.-K. Lee, H. A. M. Quinodoz, and W. N. Kreiling, Basin modeling with Basin2: A guide to using Basin2, B2plot, B2video, and B2view, Hydrogeol. Program, Univ. of Ill. at Urbana-Champaign, Urbana, 1993.

Brobst, D. A., W. P. Pratt, and V. E. McKelvey, Summary of United States mineral sources, *U.S. Geol. Surv. Circ.*, *682*, 1973.

Carpenter, A. B., Origin and chemical evolution brines in sedimentary basins, *Circ. Okla. Geol. Surv.*, *79*, 60–77, 1978.

Chapelle, F. H., *Ground-water Microbiology and Geochemistry*, John Wiley, Hoboken, N. J., 1993.

Chapelle, F. H., and L. L. Knobel, Aqueous geochemistry and the exchangeable cation compostion of glauconite in the Aquia Aquifer, Maryland, *Groundwater*, *21*, 343–352, 1983.

Clark, I., and P. Fritz, *Environmental Isotopes in Hydrogeology*, CRC Press, Boca Raton, Fla., 1997.

Connolly, C. A., L. M. Walter, H. Baadsgaard, and F. J. Longstaffe, Origin and evolution of formation waters, Alberta basin, western Canada sedimentary basin. I. Chemistry, *Appl. Geochem.*, *5*, 375–395, 1990.

Cook, M. R., *The Eutaw Aquifer in Alabama*, *Bull. Geol. Surv. Ala.*, vol. 156, 105 pp., Geol. Surv. Ala., Tuscaloosa, 1993.

Cook, M. R., Origin and evolution of anomalous hydrogeochemical character of the Tuscaloosa aquifer system of west-central Alabama, M.S. thesis, Univ. of Ala., Tuscaloosa, 1997.

Craig, H., Isotopic variations in meteoric waters, *Science*, *133*, 1702–1703, 1961.

Davis, S. N., and H. W. Bentley, Dating groundwater: A short review, in *Nuclear and Chemical Dating Techniques: Interpretation of the Environmental Record*, *ACS Symp. Ser.*, vol. 176, edited by L. A. Currie, pp. 187–222, Am. Chem. Soc., Washington, D. C., 1982.

Davis, S. N., D. O. Whittemore, and J. Fabryka-Martin, Uses of chloride/bromide ratios in studies of potable water, *Ground Water*, *36*, 338–350, 1998.

Deming, D., *Introduction to Hydrogeology*, McGraw-Hill, New York, 2002.

Dojka, M. A., P. Hugenholtz, S. K. Haack, and N. R. Pace, Microbial diversity in a hydrocarbon- and chlorinated-solvent-contaminated aquifer undergoing intrinsic bioremediation, *Appl. Environ. Microbiol.*, *64*, 3869–3877, 1998.

Domenico, P. A., and G. A. Robbins, The displacement of connate water from aquifers, *Geol. Soc. Am. Bull.*, *96*, 328–335, 1985.

Dowling, C. B., R. J. Poreda, and A. R. Basu, The groundwater geochemistry of the Bengal basin: Weathering, chemsorption, and trace metal flux to the oceans, *Geochim. Cosmochim. Acta*, *67*, 2117–2136, 2003.

Ehrlich, H. L., *Geomicrobiology*, 4th ed., Marcel Dekker, New York, 2002.

Floesser, J. A., Groundwater geochemistry of four upper Cretaceous and lower Tertiary aquifers in the Gulf Coastal Plain of southeastern Alabama, M.S. thesis, Auburn Univ., Auburn, Ala., 1996.

Freeze, R. A., and J. A. Cherry, *Groundwater*, Prentice-Hall, Old Tappan, N. J., 1979.

Garven, G., S. Ge, M. A. Person, and D. A. Sverjensky, Genesis of stratabound ore deposits in the midcontinent basins of North America, 1. The role of regional groundwater flow, *Am. J. Sci.*, *293*, 497–568, 1993.

Gelhar, L. W., C. Welty, and K. R. Rehfeldt, A critical review of data of field-scale dispersion in aquifers, *Water Resour. Res.*, *28*, 1955–1974, 1992.

Hendry, M. J., and F. W. Schwartz, An alternative view on the origin of chemical and isotopic patterns in groundwater from the Milk River aquifer, *Water Resour. Res.*, *24*, 1747–1764, 1988.

Holmen, B. A., J. D. Sison, D. C. Nelson, and W. H. Casey, Hydroxamate siderophores, cell growth and Fe(III) cycling in two anaerobic iron oxide media containing *Geobacter metallireducens*, *Geochim. Cosmochim. Acta*, *63*(2), 227–239, 1999.

Holser, W. T., Trace elements and isotopes in evaporates, *Short Coarse Notes Mineral. Soc. Am.*, *6*, 295–346, 1979.

Horton, J. W., Jr., I. Zietz, and T. L. Neathery, Truncation of the Appalachian Piedmont beneath the Coastal Plain of Alabama: Evidence from the new magnetic data, *Geology*, *12*, 51–55, 1984.

Hubbert, M. K., The theory of ground-water motion, *J. Geol.*, *48*, 785–944, 1940.

Jakobsen, R., and D. Postma, Redox zoning, rates of sulfate reduction and interactions with Fe-reduction and methanogenesis in a shallow sandy aquifer, Romo, Denmark, *Geochim. Cosmochim. Acta*, *63*, 137–151, 1999.

Johnson, T. M., R. C. Roback, T. L. McLing, T. D. Bullen, D. J. DePaolo, C. Doughty, R. J. Hunt, M. T. Murrell, and R. W. Smith, Groundwater "fast paths" in the Snake River Plain aquifer: Radiogenic isotope ratios as natural groundwater tracers, *Geology*, *28*, 871–874, 2000.

Keller, E. A., *Environmental Geology*, Prentice-Hall, Old Tappan, N. J., 2000.

King, D. T., Jr., Facies stratigraphy and relative sea-level history—Upper Cretaceous Eutaw Formation, central and eastern Alabama, *Trans. Gulf Coast Assoc. Geol. Soc.*, *40*, 381–387, 1990.

Knowles, D. B., H. L. Reade Jr., and J. C. Scott, *Geology and Groundwater Resources of Montgomery County, Alabama, With Special Reference to the Montgomery Area*, *Bull. Geol. Surv. Ala.*, vol. 68, part B, 493 pp., Geol. Surv. Ala., Tuscaloosa, 1963.

Konikow, L. F., and J. D. Bredehoeft, Modeling flow and chemical quality changes in an irrigated aquifer system, *Water Resour. Res.*, *10*, 546–562, 1974.

Lee, M.-K., Predicting diagenetic effects of groundwater flow in sedimentary basins: A modeling approach with examples, in *Basinwide Fluid Flow and Associated Diagenetic Patterns: Integrated Petrographic, Geochemical, and Hydrologic Consideration*, edited by I. P. Montanez, J. M. Gregg, and K. L. Shelton, *Spec. Publ. SEPM Soc. Econ. Paleontol. Mineral.*, *57*, 3–14, 1997.

Lee, M.-K., and C. M. Bethke, A model of isotopic fractionation in reacting geochemical systems, *Am. J. Sci.*, *296*, 965–988, 1996.

Lee, M.-K., and J. A. Saunders, Effects of pH on metals precipitation and sorption: Field bioremediation and geochemical modeling approaches, *Vadose Zone J.*, *2*, 177–185, 2003.

Lee, M.-K., and D. D. Williams, Paleohydrology of the Delaware basin, western Texas: Overpressure development, hydrocarbon migration, and ore genesis, *AAPG Bull.*, *85*, 961–974, 2000.

Lee, M.-K., J. A. Saunders, and L. W. Wolf, Effects of geologic heterogeneities on pump-and-treat and in-situ bioremediation: A stochastic analysis, *Environ. Eng. Sci.*, *17*, 183–189, 2000.

Lee, R. W., Geochemistry of groundwater in Cretaceous sediments of the southeastern coastal plain of eastern Mississippi and western Alabama, *Water Resour. Res.*, *21*, 1545–1556, 1985.

Lehmann, B. E., S. N. Davis, and J. Fabryka-Martin, Atmospheric and subsurface sources of stable and radioactive nuclides used for groundwater dating, *Water Resour. Res.*, *29*, 2027–2040, 1993.

Lovley, D. R., and F. H. Chapelle, Deep subsurface microbial processes, *Rev. Geophys.*, *33*, 365–381, 1995.

Lovley, D. R., F. H. Chapelle, and E. J. P. Phillips, Fe(III)-reducing bacteria in deeply buried sediments of the Atlantic coastal plain, *Geology*, *18*, 954–957, 1990.

Madigan, M. T., J. M. Martinko, and J. Parker, *Biology of Microorganisms*, Prentice-Hall, Old Tappan, N. J., 1996.

Madsen, E. L., Nucleic-acid characterization of the identity and activity of subsurface microorganisms, *Hydrogeol. J.*, *8*, 112–125, 2000.

Malhotra, S., A. S. Tankhiwale, A. S. Rayvaidya, and R. A. Pandey, Optimal conditions for bio-oxidation of ferrous ions to ferric ions using *Thiobacillus ferrooxidans*, *Biores. Tech.*, *85*, 225–234, 2002.

Miller, J. A., *Ground Water Atlas of United States: Alabama, Georgia, and Florida, Hydrol. Invest. Atlas HA 730-G*, U.S. Geol. Surv., Reston, Va., 1990.

Miller, S. C. M., J. J. LiPuma, and J. L. Parke, Culture-based and non-growth-dependent detection of the *Burkholderia cepacia* complex in soil environments, *Appl. Environ. Microbiol.*, *68*, 3750–3758, 2002.

Person, M. E., and G. Garven, A sensitivity study of the driving forces on fluid flow during continental-rift basin evolution, *Geol. Soc. Am. Bull.*, *106*, 461–475, 1994.

Person, M., J. P. Raffensperger, S. Ge, and G. Garven, Basin-scale hydrologic modeling, *Rev. Geophys.*, *34*, 61–87, 1996.

Ranganathan, V., and J. S. Hanor, A numerical model for the formation of saline waters due to diffusion of dissolved NaCl in subsiding sedimentary basins with evaporites, *J. Hydrol.*, *92*, 97–120, 1987.

Raymond, D. E., and C. W. Copeland, Selected columnar sections for the Coastal Plain, Appalachian Plateaus, Interior Low Plateaus, and Valley and Ridge Provinces in Alabama, *Geol. Surv. Ala. Atlas Ser.*, *20*, 43 pp., 1987.

Raymond, D. E., W. E. Osborne, C. W. Copeland, and T. L. Neathery, Alabama stratigraphy, *Circ. Geol. Surv. Ala.*, *140*, 97 pp., 1988.

Roback, R. C., T. M. Johnson, T. L. McLing, M. T. Murrell, S. Luo, and T.-L. Ku, Uranium isotopic evidence for groundwater chemical evolution and flow patterns in the eastern Snake River Plain aquifer, Idaho, *Geol. Soc. Am. Bull.*, *113*, 1133–1141, 2001.

Roden, E. E., M. R. Leonardo, and F. G. Ferris, Immobilization of strontium during iron biomineralization coupled to dissimilatory hydrous ferric oxide reduction, *Geochim. Cosmochim. Acta*, *66*, 2823–2839, 2002.

Saunders, J. A., M. A. Prichett, and R. B. Cook, Geochemistry of biogenic pyrite and ferromanganese stream coatings: A bacteria connection?, *Geomicrobiol. J.*, *14*, 203–217, 1997.

Scott, J. C., R. H. Cobband, and D. Castleberry, Geohydrology and susceptibility of major aquifers to surface contamination; area 8, *U.S. Geol. Surv. Water Resour. Invest. Rep., 86-4360*, 65 pp., 1987.

Small, T. D., L. A. Warren, E. E. Roden, and F. G. Ferris, Sorption of strontium by bacteria, Fe(II) oxide and bacteria-Fe(III) oxide composites, *Environ. Sci. Technol.*, *33*, 4465–4470, 1999.

Stueber, A. M., and L. M. Walter, Origin and chemical evolution of formation waters from Silurian-Devonian strata in the Illinois basin, USA, *Geochim. Cosmochim. Acta*, *55*, 309–325, 1991.

Wheatcraft, S. W., and S. W. Tyler, An explanation of scale-dependent dispersivity in heterogeneous aquifer using concepts of fractal geometry, *Water Resour. Res.*, *24*, 566–578, 1988.

Zobrist, J., P. R. Dowddle, J. A. Davis, and R. S. Oreland, Mobilization of arsenite by dissimilatory reduction of absorbed arsenate, *Environ. Sci. Technol.*, *31*, 4646–4753, 2000.

M.-K. Lee and E. Penny, Department of Geology and Geography, 210 Petrie Hall, Auburn University, AL 36849, USA. (leeming@mail.auburn.edu)

C. Morton, Carnegie Museum of Natural History, 4400 Forbes Avenue, Pittsburgh, PA 15213, USA.